Infiltration of Fiber Preforms by an Alloy: Part III. Die Casting Experiments

P. JARRY, V.J. MICHAUD, A. MORTENSEN, A. DUBUS, and R. TIRARD-COLLET

Preforms of 20 vol pct SAFFIL alumina fibers are infiltrated with Al-4.4 wt pct Cu-0.3 wt pct Mg using a horizontal die casting machine. Fiber preform temperature is varied from 973 to 673 K. Solute distribution, fiber volume fraction, and matrix microstructure are characterized using optical metallography and electron microprobe analysis. Increases in fiber volume fraction are observed in the composites downstream of the infiltration path. We propose that these result from locking of the compressed fibers by solid metal present during infiltration. With this assumption, we find good agreement between theory presented in Parts I[1] and II[2] for solute concentration, fiber volume fraction distributions, as well as matrix microstructure and experiments. With an initial preform temperature of 673 K, freckles are found in the composite, which are interpreted to result from the combined effects of pressure and significant enrichment in solute at the infiltration front.

I. INTRODUCTION

PRESSURE casting offers considerable potential for producing fiber-reinforced metals: adverse wetting is overcome and shrinkage pores are eliminated in a process that allows for high production rates. As in most casting operations, process parameters significantly influence the final macro- and microstructure of the resulting material in a way that must be understood before the process can be used in a reliable and optimized fashion.

In two previous articles[1,2] (hereafter referred to as Part I and Part II, respectively), two of the present authors presented an analysis of the unidirectional infiltration of fiber preforms by a binary alloy. It was shown that when the initial fiber preform temperature is below the metal liquidus, solid metal forms in the composite during infiltration. This solidification phenomenon induces substantial macrosegregation and variations in grain size within the composite and strongly influences infiltration kinetics. The analysis was in good agreement with experimental data generated by infiltrating alumina fiber preforms with Al-4.5 wt pct Cu using an apparatus which allows infiltration under constant applied pressure with independent control of all process parameters.

In this article, we present results from experiments on the pressure casting of aluminum-based alloys into chopped alumina fiber preforms in which the apparatus and procedures are less accurately controlled but replicate industrial processing conditions. We vary the initial fiber temperature T_f, analyze microstructure and macrosegregation in the final composite, and investigate the applicability of theoretical analysis for the present casting conditions.

P. JARRY, Research Engineer, A. DUBUS, Research Engineer, and R. TIRARD-COLLET, Technical Staff Member, are with the Centre de Recherches Pechiney, 38340 Voreppe, France. V.J MICHAUD, Postdoctoral Research Associate, and A. MORTENSEN, Associate Professor, are with the Department of Materials Science and Engineering, Massachusetts Institute of Technology, Cambridge, MA 02139.

Manuscript submitted August 13, 1991.

II. EXPERIMENTAL PROCEDURE

The fiber preforms were SAFFIL* δ-alumina preforms, 30 mm-thick and 120 mm in diameter, with an initial fiber volume fraction of 20 pct, essentially similar to those used and described in more detail in Part II.[2] Preform cohesion was ensured by the use of a few weight percent silica binder. The matrix was aluminum alloy AU5GT (4.4 wt pct Cu, 0.27 wt pct Mg, 0.18 wt pct Ti, <0.02 wt pct impurities, balance Al). The pressure casting apparatus was a horizontal shot-chamber die casting machine in which the fiber preform was held vertically against the die wall opposite the shot chamber (Figure 1). The fiber preforms were preheated to a chosen temperature (T_f) in a separate furnace and inserted into the die chamber. Metal was then poured at 1070 K into the shot chamber and forced by a piston into the die. The time elapsed between retrieval of the preform from the preheating furnace and infiltration was on the order of 20 seconds. The initial mold temperature was between 470 and 570 K depending on location within the mold. Separate investigations at Centre de Recherches de Voreppe SA (CRV) showed that by the time the metal penetrates the preform, it has cooled to a temperature of about 970 K.

*SAFFIL is a trademark of IC1 Americas, Inc., Wilmington, DE.

Four composite castings were produced, in which the fiber preforms were initially preheated to T_f = 973, 873, 773, and 673 K (samples A, B, C, and D, respectively). A casting similar to these samples but containing no fiber preform, designated as sample E, was also produced. Finally, data are also presented from a smaller composite casting, produced similarly with T_f = 623 K but using a different mold, which is designated as sample F.

Samples were cut from the center of castings A through E, where infiltration was unidirectional toward the die wall. These samples were then solutionized for 8 hours at 798 K and quenched in water in order to eliminate microsegregation within the matrix. They were then polished, to be examined first under an optical microscope, then using an analytical scanning electron microscope

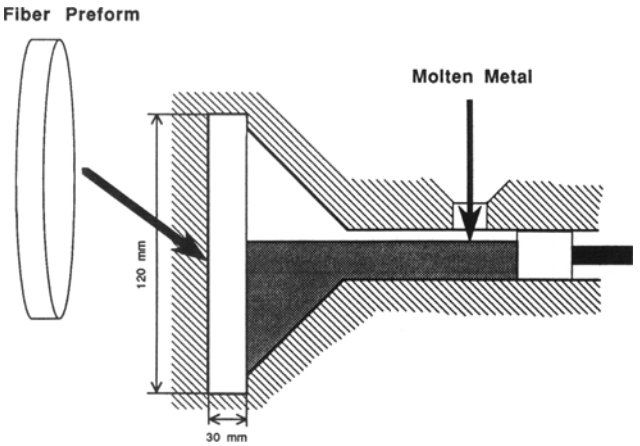

Fig. 1 — Schematic diagram of the die casting apparatus.

(ASEM). The ASEM is composed of a scanning electron microscope equipped with a LaB_6 filament operated in the back-scattered electron (BSE) mode. It is interfaced with an energy-dispersive X-ray microanalyzer (EDX) and with an automated image analyzer. The latter drives both the SEM functions (stage, beam, magnification) and the EDX acquisition routines.

The local surface fraction of fibers was measured with the image analyzer using a high sensitivity BSE detector to enhance contrast between the (darker) fibers and the matrix. A relatively low acceleration voltage (15 kV) was used to maintain the fiber-matrix interface as sharp as possible. A mask, comprising the fibers enlarged by a shadow 2-μm wide, was then created in the image analyzer. This was used to guide the electron beam away from the fibers in order to scan only the remainder of the sampled area during chemical analysis by EDX. This procedure ensured that signal only originated from the matrix during analysis. Data were collected in this manner from square areas of side 200 μm once every millimeter along the infiltration direction to yield the concentration in Al, Cu, and Si. The acceleration voltage was 15 kV, the primary beam current was $1.5 \cdot 10^{-10}$ A, and data acquisition times varied from 100 to 200 seconds per field.

III. EXPERIMENTAL RESULTS

In the fiber-free control sample E, the metal microstructure is composed of a columnar region about 5- to 7-mm wide along the die wall, containing large grains about 1 mm in diameter (Figure 2). Moving from this region toward the piston, the metal is thereafter composed of equiaxed grains of size decreasing gradually from 1000 to 250 μm.

Composite samples A through D are well infiltrated, except in a zone near the die wall opposite the shot chamber. The width of this zone is less than 1 mm in samples A through C and between 1 and 2 mm in sample D.

Macrostructural investigation of the composites shows several regions along the direction of infiltration differing by grain size, fiber volume fraction V_f, and composition. In sample A (Figure 3(a)), moving from the die wall toward the piston, a narrow fine-grained zone about 1-mm wide along the die wall is first encountered, followed by a columnar zone of grains about 100-μm wide and orthogonal to the die wall, which extends 9 mm into the composite. The remainder of the composite matrix and the unreinforced region consist of equiaxed grains of average diameter, around 250 μm in the composite and several millimeters in the unreinforced matrix. In samples B through D (Figures 4(a), 5(a) and 6(a) respectively), a fine-grained equiaxed region is found first along the die wall. The average grain size in this region, on the order of 10 to 20 μm, is only apparent at higher magnification (Figure 7(a)). Within this fine-grained equiaxed region located near the die wall, the fiber volume fraction V_f is significantly higher than the nominal 20 pct of the preforms (Figures 4(b), 5(b), 6(b), and 7(a)) (in sample D, measurement of V_f is affected by porosity because the mask in the image analyzer counts dark pores as fibers). Correspondingly, the composite width is decreased below the initial preform width of about 30 mm after infiltration (Table I). In the remainder of the

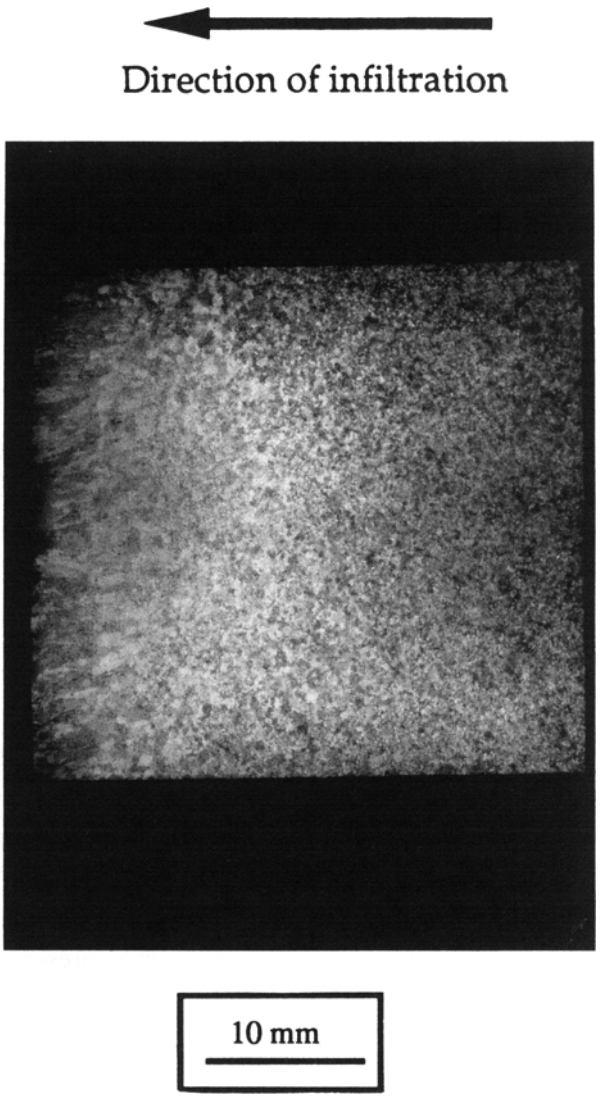

Fig. 2 — Macrostructure of sample E (no preform).

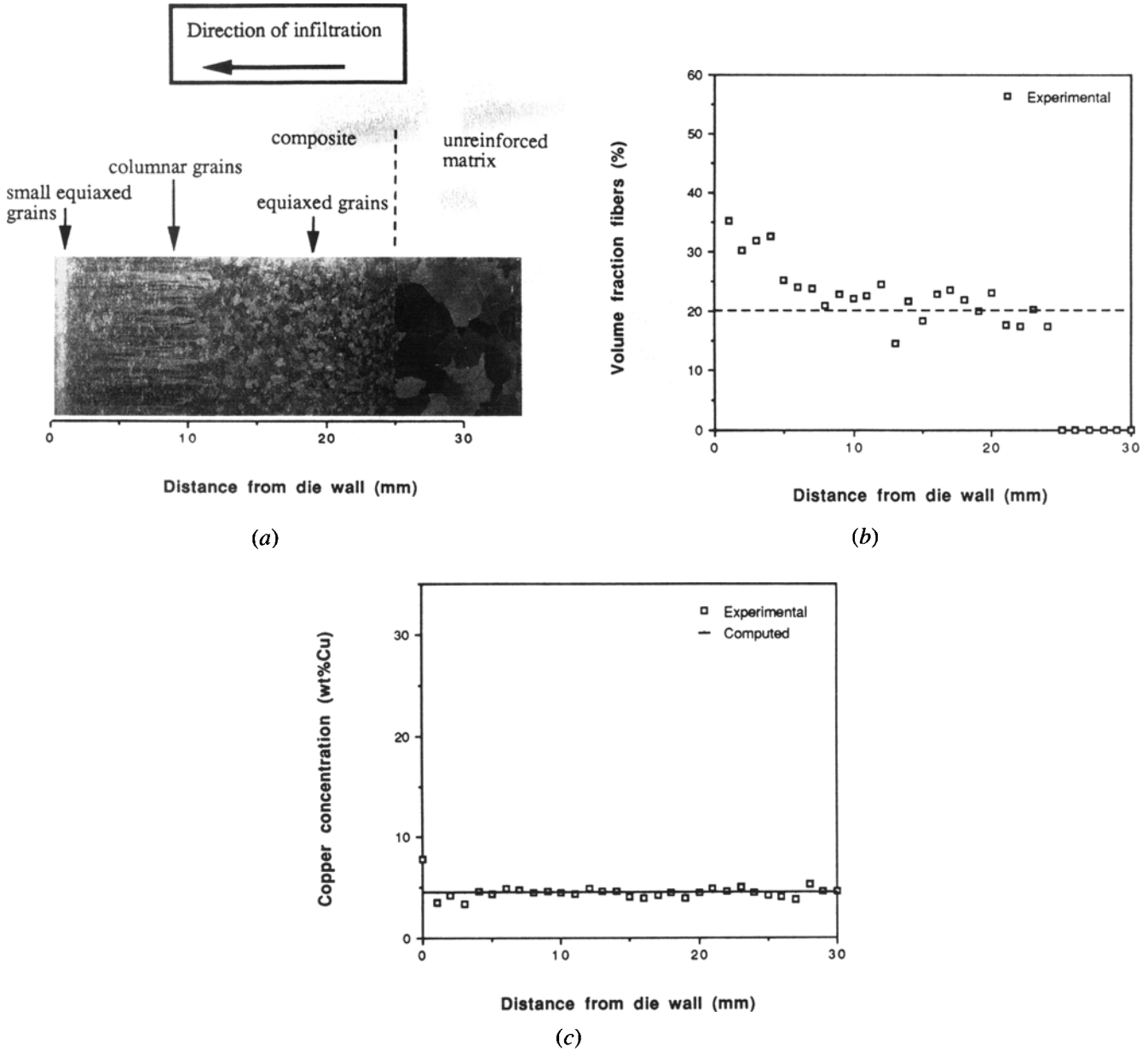

Fig. 3—(*a*) Macrostructure, (*b*) fiber volume fraction, and (*c*) matrix copper content (predicted and measured), as a function of distance from the die wall, for sample A (T_f = 973 K). The abscissa axis of the plots matches horizontal distance along the macrograph.

composites, V_f is close to its nominal value of 20 pct and the matrix is composed of larger equiaxed grains of size increasing roughly in order of magnitude from about 10^2 to 10^3 μm toward the piston (Figures 4(a) and (b), 5(a) and (b), 6 (a) and (b), and 7(b)). In the unreinforced region near the piston, the alloy grains are equiaxed and of variable size above about 250 μm (Figures 4(a), 5(a), and 6(a)). In sample D (Figure 6(a)), a large-grained zone is also included within the fine-grained region near the die wall.

Results from quantitative analysis of matrix composition are given in Figures 3(c), 4(c), 5(c), and 6(c). General features of macrosegregation are qualitatively similar in all four samples, although they differ from a quantitative standpoint. In all composites, the matrix is enriched in copper near the die wall. In this region, second phases, which include copper-rich intermetallics and silicon, are concentrated in the vicinity of the fiber/matrix interface. Moving toward the piston from the die wall, a second region of copper composition lower than the nominal matrix composition is then found. Next, on the preform side facing the piston, the copper concentration equals that of the starting alloy. This third region of nominal copper concentration is identical to that of nominal fiber volume fraction (20 pct) (Figures 3(b) and (c), 4(b) and (c), 5(b) and (c), and 6(b) and (c)). The width of this third region decreases with decreasing T_f. Additionally, near the periphery of the reinforced portion of sample D, veins of high copper concentration emanate from the first, copper-rich region, along the die

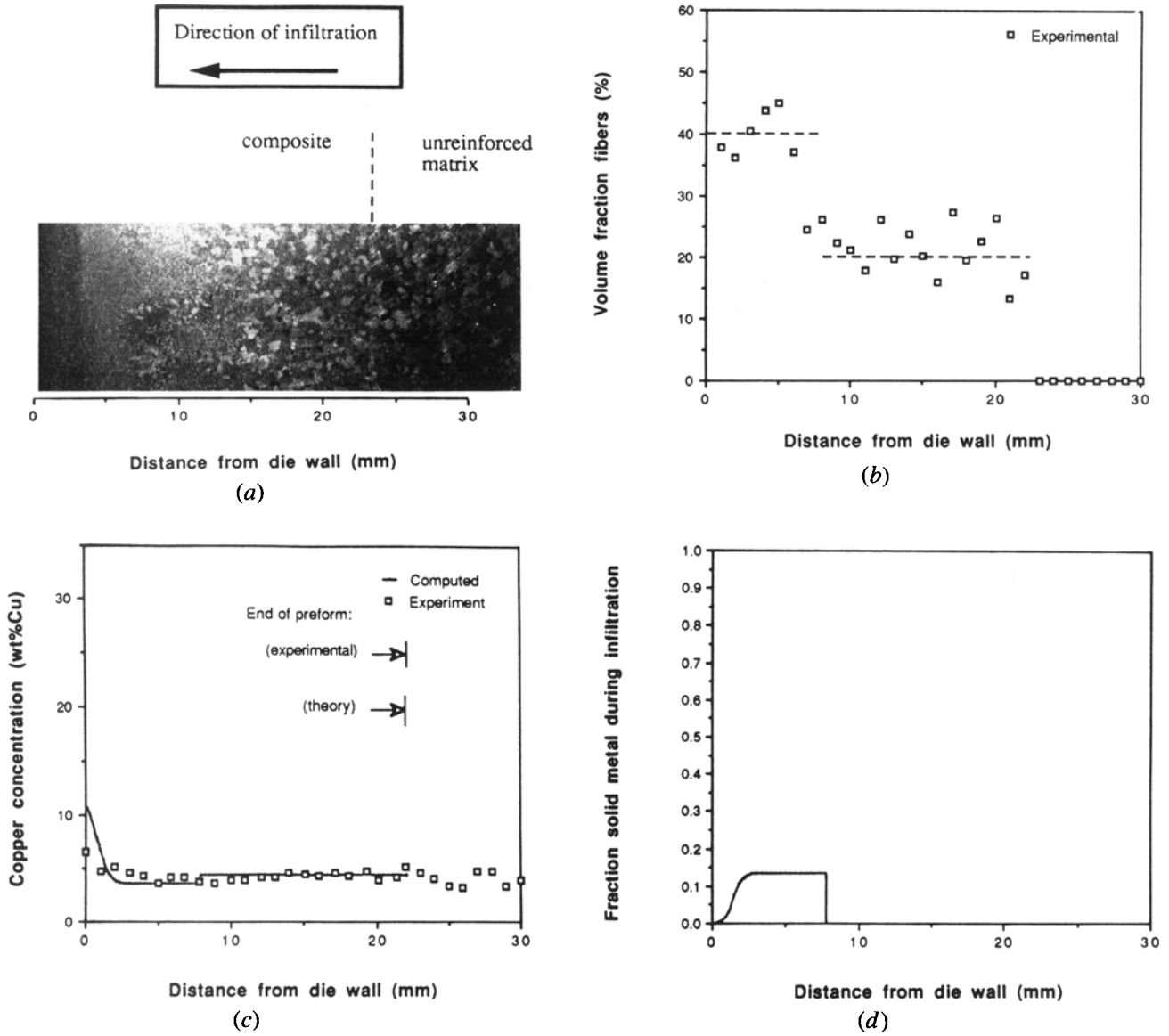

Fig. 4—(*a*) Macrostructure, (*b*) fiber volume fraction, (*c*) matrix copper content (predicted and measured), and (*d*) calculated fraction solid, as a function of distance from the die wall, for sample B (T_f = 873 K). The abscissa axis of the plots matches horizontal distance along the macrograph.

wall. These extend radially toward the lateral die walls (Figures 8 and 9).

IV. DISCUSSION

Increases in fiber volume fraction V_f above the nominal preform value have been observed previously in squeeze cast fiber or whisker-reinforced aluminum by several other investigators[3–7]. This effect results from preform compression, induced during infiltration by the flowing pressurized metal *via* viscous drag and capillary forces.[7] These forces transmit the full applied pressure to the preform ahead of the infiltration front and lead to gradual local relaxation of the preform as infiltration progresses.[7] After the preform is fully infiltrated, metal flow stops, so these forces decay to zero. The preform then relaxes to a state of zero stress, where the matrix is fully liquid.[7] Where solid metal has formed during infiltration, on the other hand, relaxation of the preform may be prevented, both during and after infiltration.

It was shown in Part I[1] that when T_f is lower than the metal liquidus, a region (defined as region 1) in which the matrix is semisolid, forms near the infiltration front. This region is separated by a region of nominal composition (defined as region 3) from that portion of the preform surface where molten superheated metal penetrates the preform. Region 3 forms because solid metal formed previously is remelted by the incoming superheated metal. The close correspondence between the point of transition from low to high V_f and that of the transition from nominal matrix composition to a copper-depleted matrix indicates that the preforms remained compressed in region 1, while they relaxed in region 3. The increased V_f near the die wall would then be due to locking by solid metal in region 1 of the fibers in the

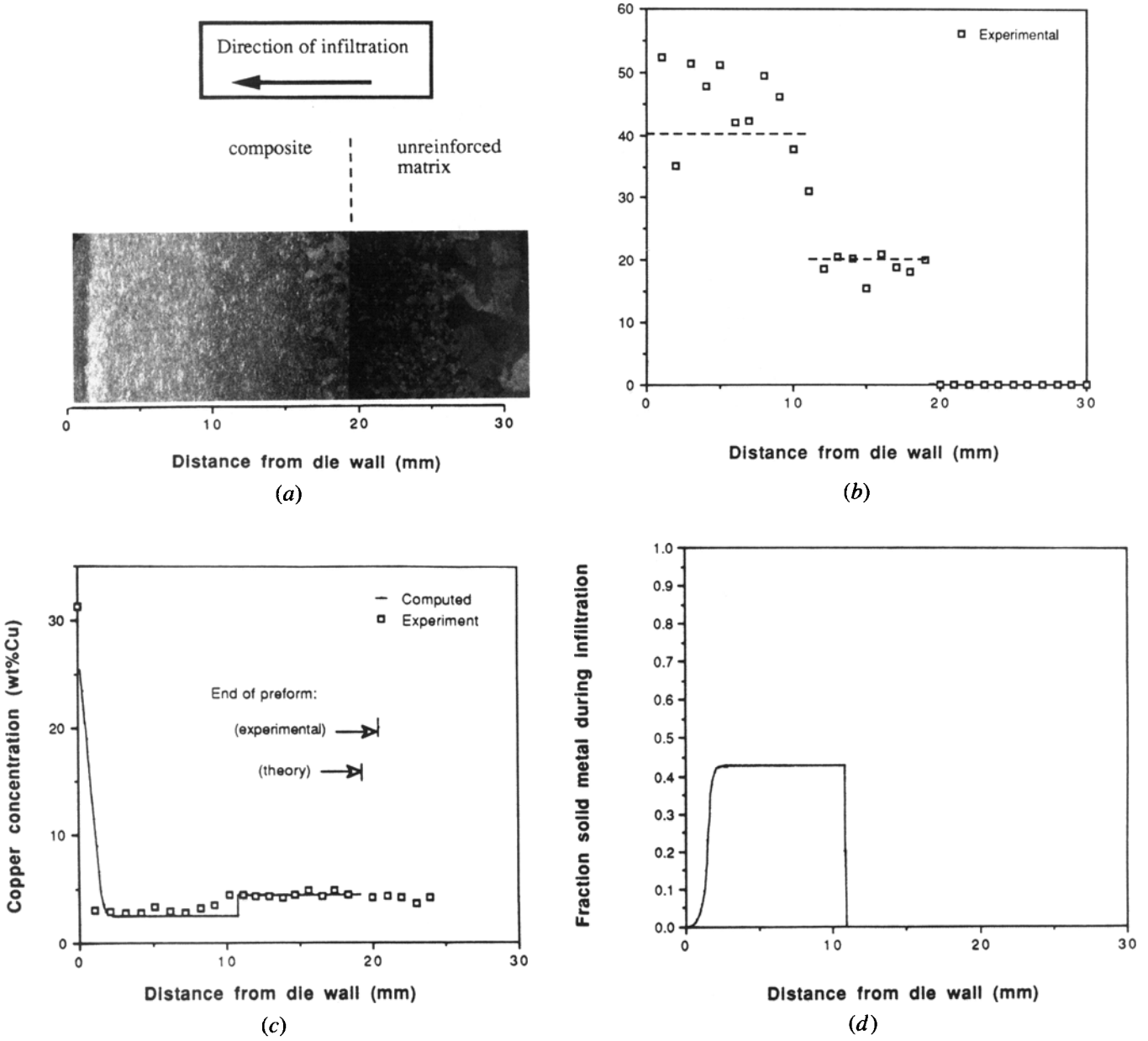

Fig. 5—(*a*) Macrostructure, (*b*) fiber volume fraction, (*c*) matrix copper content (predicted and measured), and (*d*) calculated fraction solid, as a function of distance from the die wall, for sample C (T_f = 773 K). The abscissa axis of the plots matches horizontal distance along the macrograph.

compressed state experienced by the preform at the infiltration front. Remelting of solid metal at the interface between regions 1 and 3 then allows the preform to relax both during infiltration and when flow ceases.

With this interpretation of variations in V_f, longitudinal macrosegregation in the central portion of composite samples B through D can be modeled using the theory of adiabatic unidirectional infiltration developed in Part I.[1] Infiltration is roughly adiabatic in the analyzed regions because (1) external cooling by the lateral die walls is of no consequence in the central portion of the composite (infiltration lasts less than 5 seconds, and the thermal diffusivity of the composite is about $2 \cdot 10^{-5}$ $m^2\ s^{-1}$,[8,9] and (2) conduction ahead of the infiltration front into the preform is negligibly small.

The model for unidirectional infiltration developed in Part I[1] assumes that the applied pressure is constant, in which case the infiltration front progresses as $\psi \cdot \sqrt{t}$, where ψ is a constant and t is time. In the present infiltration experiments, the metal was not driven under constant pressure. In applying the analysis of Part I[1] to the present data, therefore, we neglect the influence of variations of the applied pressure and roughly estimate ψ as the square root of the product of the average metal velocity during infiltration by the length of the sample. This yields $\psi = 0.022\ m \cdot s^{-1/2}$ for all four samples A through D. The sensitivity of theoretical results to ψ was investigated within its range of plausible values and found to be small. Also, the matrix, which contains some Mg and Si, is approximated as a binary Al-4.4 wt pct Cu alloy.

Because the analysis in Part I[1] was developed for constant V_f, we assume here that V_f during infiltration

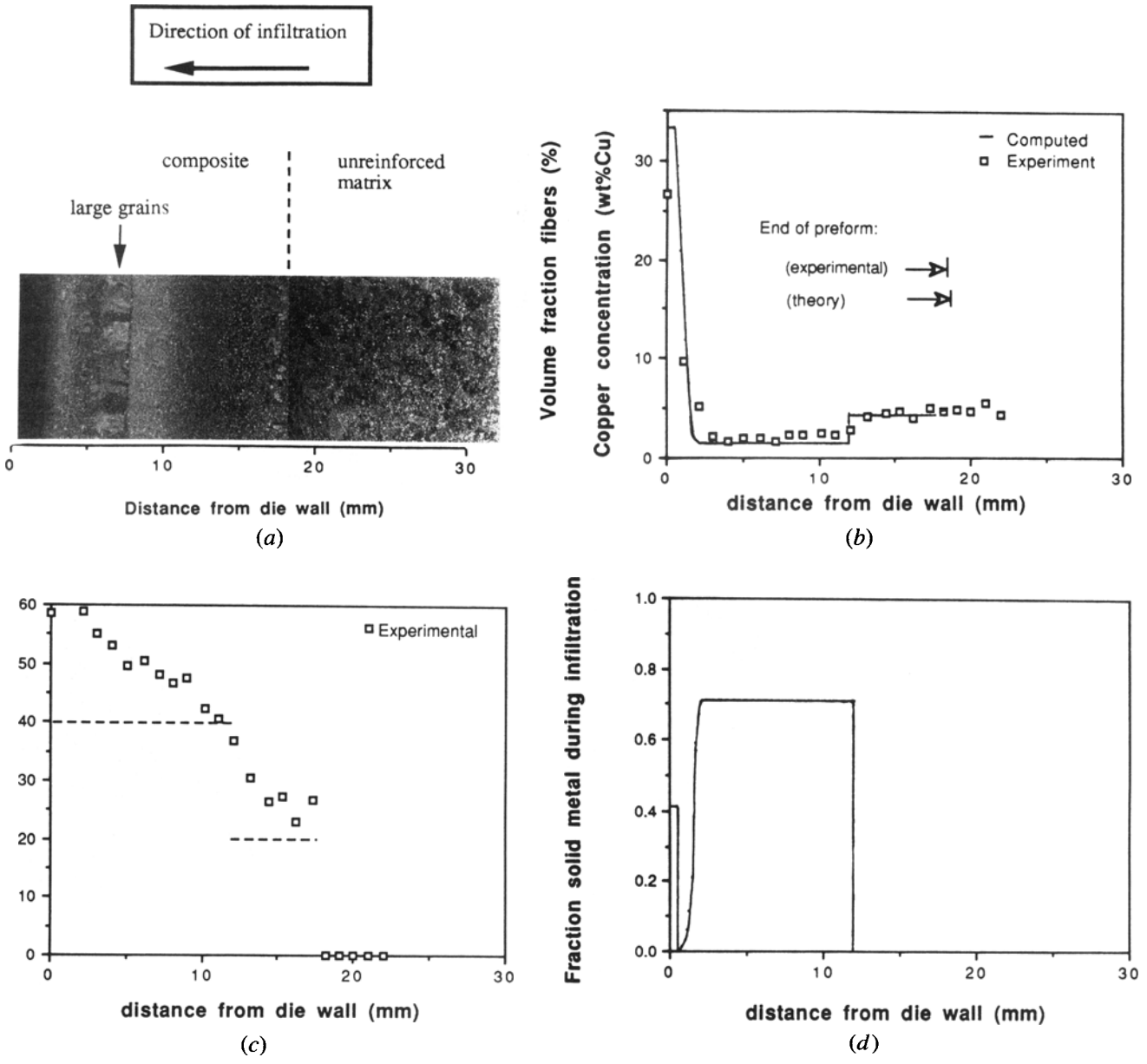

Fig. 6—(*a*) Macrostructure, (*b*) fiber volume fraction, (*c*) matrix copper content (predicted and measured), and (*d*) calculated fraction solid, as a function of distance from the die wall, for sample D (T_f = 673 K). The abscissa axis of the plots matches horizontal distance along the macrograph.

corresponds everywhere to that of the compressed preform at the infiltration front. We thus take V_f = 40 pct, a value selected using results from microprobe analysis of the compressed portions of the composites (Figures 4(b), 5(b), and 6(b)). This assumption is realistic in region 1 (which predominantly governs fluid flow because of its much lower permeability) because metallographic data show that solid metal holds the fibers together; however, we know that during infiltration, V_f varies over the length of region 3 because of gradual relaxation of the preform in the absence of solid metal.[7]

When infiltration stops, region 3 of the preform relaxes to attain a uniform value of V_f corresponding to an unstressed condition following the deformation it has experienced during infiltration. From data in Figures 4(b), 5(b), and 6(b), this value is near 20 pct. Having applied the model of Part I[1] with V_f = 40 pct, we then expanded region 3 of the composite by decreasing V_f from its compressed value (of 40 pct) to that of the fully relaxed preform (20 pct). From these final values of V_f in region 3 after relaxation and from the predicted remelting front position in the fully compressed preform, the final composite length is thus predicted.

Calculated solute and fraction solid metal profiles are plotted in Figures 4 through 6, in plots (c) and (d), respectively. Agreement is satisfactory, with respect to copper content, position of the remelting front, and final composite width.

Theory predicts no segregation for sample A, because T_f is greater than the matrix liquidus. This agrees with experiment, except in a thin layer near the die wall, downstream of the infiltration path, which features

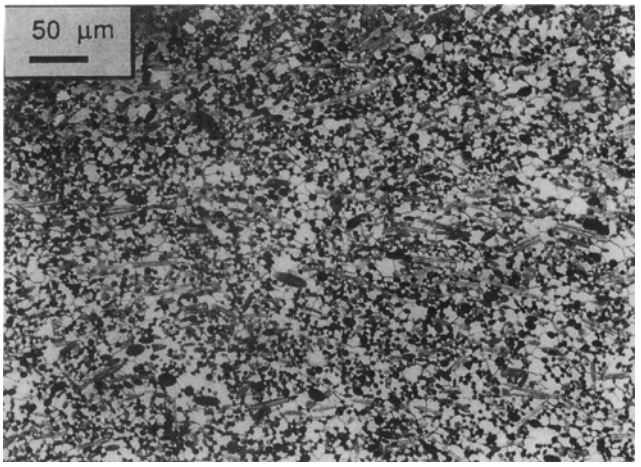

(*a*)

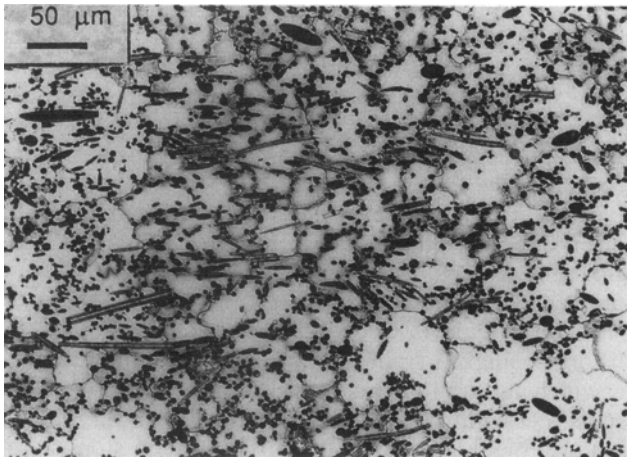

(*b*)

Fig. 7—Microstructure of two different zones in sample B (T_f = 873 K) revealed by Keller's etch. (*a*) is taken in the zone of high volume fraction fibers and (*b*) is taken in the zone where the volume fraction fiber is close to nominal.

variations in copper content and fiber volume fraction. We interpret these localized variations in composition and fiber volume fraction as resulting from cooling of the preform against the die wall before infiltration. Estimating the preform thermal diffusivity α as $4 \cdot 10^{-7}$ $m^2 \cdot s^{-1}$[8,9] and using the usual error function solution for the temperature profile in the preform before infiltration, the liquidus isotherm T = 923 K penetrates about 6 mm

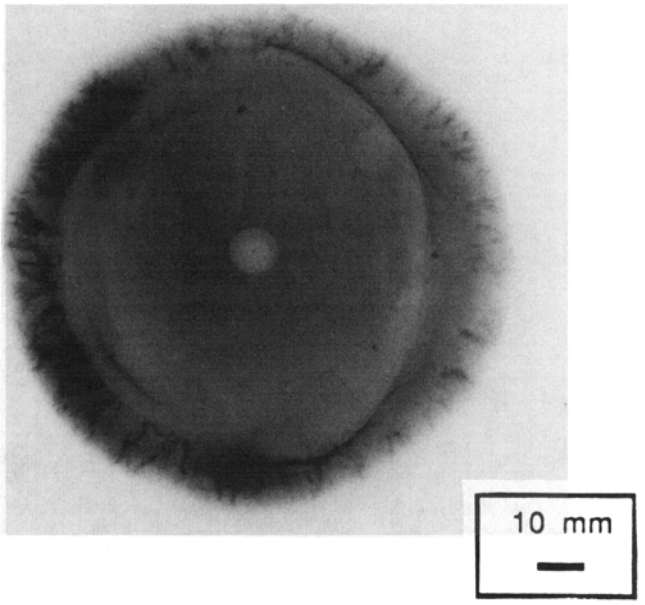

Fig. 8—Radiograph of sample D (T_f = 673 K), showing veins extending radially toward the circumferential walls.

into the preform during the time interval between placement of the preform into the die and infiltration, 20 seconds. This is of the same order of magnitude as the observed segregated zone length in sample A, which is 5 mm. Local solidification of the metal in the cooled layer of the preform can, therefore, account for segregation and increased V_f in the composite near the die wall when T_f is above the matrix liquidus.

As in Part II[2], the fine grains observed in samples B through D are explained by the solidification that took place during infiltration. The fine-grained equiaxed regions of these samples extend farther than the solute-depleted and fiber-enriched regions of the composite, interpreted as region 1 of the model. This was not observed in samples produced in Part II using lower infiltration pressures and featuring no preform compression. The finer grain sizes found in region 3 near the remelting front separating region 3 from region 1 could be interpreted knowing from theory that the local temperature decreases within region 3 from the metal inlet to the remelting front (see Figures 1, 7, and 8 of Reference 1). Experimental data of Das *et al.*[10] show that under an applied pressure of 110 MPa (of the same order of magnitude as pressures used in this work), the grain size of Al-4 pct Cu decreases sharply with decreasing metal initial temperature. In sample A, the macrostructure is similar to that

Table I. List of Samples and Changes in Preform Dimensions

Sample	T_f (K)	Initial Preform Width (mm)	Final Preform Width (mm)	Pct Preform Deformation
A	973	30.2	24	20
B	873	30.2	22	27
C	773	30.4	20.5	33
D	673	30	>17	<43
E	—	0	0	—
F	623	(different geometry)	(different geometry)	(different geometry)

Fig. 9—Microstructure of sample D (T_f = 673 K), revealed by Keller's etch, showing freckles emanating from the solute-rich region.

with no preform in the die (sample E), save for the equiaxed zone near the die wall. This zone was formed in sample A, as in samples B through D, because of cooling by the fibers (and is, therefore, not the chill zone encountered in ordinary castings). The larger extent of the columnar zone in sample A compared to that of sample E probably results from the fact that fibers inhibit convection of the molten metal. It is well known that convection in castings favors grain multiplication and, hence, the presence of a central equiaxed zone.[11] Cole and Bolling[12] demonstrated this effect in casting experiments in which metallic grids were placed in the mold to reduce convective flow in the liquid. Overall trends in composite structure observed here are therefore similar to those observed previously by Clyne and Mason[13] and by two of the present authors in Part II,[2], and agree quantitatively with theory presented in Parts I and II.

The presence of silicon in the matrix is an indication that the fibers (which contain 4 pct SiO_2) or the silica binder used in preparing the preforms is reduced by the matrix. This agrees with Reference 14, in which small amounts of silicon were detected near the interface in composites of SAFFIL preforms infiltrated with pure aluminum. The presence of magnesium in the infiltrating alloy probably accelerates this reaction, because no silicon was visible under the optical microscope in similar composites produced with binary Al-4.5 wt pct Cu in Part II.[2]

The copper-rich matrix veins in sample D resemble narrow solute-rich channels found in unreinforced castings and known as freckles. These are known to result from flow instabilities which arise in semisolid regions when the isotherm velocity is lower than the velocity of interdendritic fluid.[15–21] When solute-rich liquid penetrates solute-poor semisolid regions, solid primary metal remelts because of the increase in local liquid composition. In regions where more melting has occurred, resistance to flow is lowest, so flow of the solute-rich liquid is locally eased. This, in turn, induces more remelting, producing solute-rich veins in the final sample microstructure. Figure 9 indicates that in sample D, freckle formation was induced by flow of solute-rich liquid initially located along the die wall opposite the gate. Backflow of this liquid near the outer wall could be explained by matrix shrinkage due to rapid cooling near the peripheral die wall and by the fact that pressure is applied only directly to the center of the preform, its periphery being indirectly connected to the gate (Figure 1). These causes explain both the shape and the location of the freckles in sample D. The absence of such freckles in other samples must have resulted from the lower level of solute enrichment at the infiltration front and the lower amount of solid matrix in region 1 of these samples, which lower the effect of local remelting on the rate of liquid flow.

Large equiaxed grains found in the center of sample F, in which infiltration was from all sides and infiltration fronts met within the preform (Figure 10), is an illustration of remelting occurring when infiltration stops in region 1 due to equilibration of temperature gradients, a phenomenon modeled and observed in Part II.[2] A similar structure can also be observed in experiments by Chadwick (Figure 5 of Reference 22), in which a SAFFIL preform was infiltrated by an aluminum alloy from all sides. Some features of the matrix microstructure in sample D, where a large-grained zone is also found between two fine-grained zones, are, however, not explained by the analysis in Parts I[1] and II.[2]

V. CONCLUSIONS

1. Significant variations in fiber volume fraction and matrix grain size and composition are observed in SAFFIL alumina short fiber preforms initially at a volume fraction of 20 pct infiltrated by aluminium alloy AU5GT under a maximum applied pressure on the order of 70 MPa in casting equipment and procedures typical of industrial practice.
2. A portion of the preforms was significantly deformed after infiltration. This is interpreted as a joint result of preform compression by the pressurized infiltrating metal and formation of solid metal between the fibers during infiltration, which prevents the relaxation of compressed preforms when infiltration stops. This results in variations in fiber volume fraction within the final solidified composite.

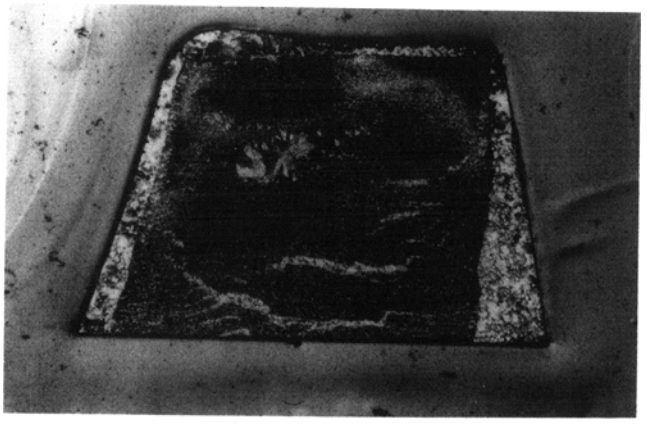

(*a*)

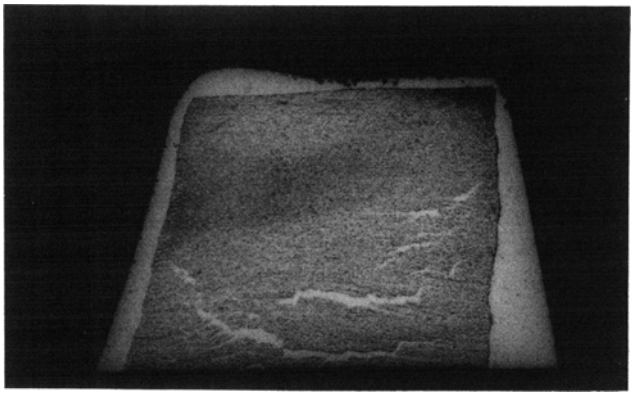

(*b*)

Fig. 10—(*a*) Large equiaxed grains revealed by Keller's etch in the central part of sample F (the large-grained region is slightly to the upper left of the sample's center); (*b*) is the same plane of polish as (a), but after nitric etching: an increased copper concentration in the region that contained large grains in (a) is revealed by a darker coloration.

3. After modification to account for fiber preform compression, the theoretical analysis presented in Parts I[1] and II[2] successfully predicts macrosegregation, the locations of changes in fiber volume fraction, and overall microstructure in the infiltrated composites.
4. Freckles formed in the composite near the lateral die wall when the initial fiber temperature was 673 K. These are interpreted as resulting from backflow of copper-rich liquid located initially downstream of the infiltration path.

ACKNOWLEDGEMENTS

We want to thank M. Chastagnier for the ASEM analysis and M.M. Pluchon and Burtin for fabricating the composite materials at CRV workshops. This work was funded by the Centre de Recherches de Voreppe, SA.

REFERENCES

1. A. Mortensen and V. Michaud: *Metall. Trans. A*, 1990, vol. 21A, pp. 2059-72.
2. V.J. Michaud and A. Mortensen: *Metall. Trans. A*, 1992, vol. 23A, pp. 2263-80.
3. T. Imai, Y. Nishida, M. Yamada, H. Matsubara, and I. Shirayanagi: *J. Mater. Sci. Lett.*, 1987, vol. 6, pp. 343-45.
4. H. Fukunaga: *Int. Symp. on Advances in Cast Reinforced Metal Composites*, Proc. Conf., Chicago, IL, S.G. Fishman and A.K. Dhingra, eds., ASM INTERNATIONAL, Materials Park, OH, 1988, pp. 101-07.
5. Y. Nishida, H. Matsubara, M. Yamada, and T. Imai: *4th Japan–U.S. Conf. on Composite Materials*, Proc. Conf., Washington, DC, Technomic Publishing Co., Lancaster, PA, 1988, pp. 429-38.
6. N.W. Rasmussen, P.N. Hansen, and S.F. Hansen: *Mater. Sci. Eng.*, 1991, vol. A135, pp. 41-43.
7. J.L. Sommer: Ph.D. Thesis, Massachusetts Institute of Technology, Cambridge, MA, 1992.
8. A. Mortensen, L.J. Masur, J.A. Cornie, and M.C. Flemings: *Metall. Trans. A*, 1989, vol. 20A, pp. 2535-47.
9. L.J. Masur, A. Mortensen, J.A. Cornie, and M.C. Flemings: *Metall. Trans. A*, 1989, vol. 20A, pp. 2549-57.
10. A.A. Das, A.J. Clegg, B. Zantout, and M.M. Yakoub: *Int. Symp. on Advances in Cast Reinforced Metal Composites*, Proc. Conf., Chicago, IL, S.G. Fishman and A.K. Dhingra, eds., ASM INTERNATIONAL, Materials Park, OH, 1988, pp. 139-47.
11. G.J. Davies: *Solidification and Casting*, Halsted Press, John Wiley & Sons, New York, NY, 1973, pp. 95-115.
12. G.S. Cole and G.F. Bolling: *Trans. AIME*, 1965, vol. 233, pp. 1568-72.
13. T.W. Clyne and J.F. Mason: *Metall. Trans. A*, 1987, vol. 18A, pp. 1519-30.
14. Q. Li, D.C. Dunand, A. Mortensen, and J.A. Cornie: *Metall. Trans. A*, 1991, vol. 22A, pp. 1126-28.
15. M.C. Flemings: *Solidification Processing*, McGraw-Hill, New York, NY, 1974.
16. Anthony F. Giamei and B.H. Kear: *Metall. Trans.*, 1970, vol. 1, pp. 2185-92.
17. S.M. Copley, Anthony F. Giamei, S.M. Johnson, and M.F. Hornbecker: *Metall. Trans.*, 1970, vol. 1, pp. 2193-2204.
18. R.J. McDonald and J.D. Hunt: *Metall. Trans.*, 1970, vol. 1, pp. 1787-88.
19. R.J. McDonald and J.D. Hunt: *Trans. AIME*, 1969, vol. 245, pp. 1993-97.
20. R. Mehrabian, M.A. Keane, and M.C. Flemings: *Metall. Trans.*, 1970, vol. 1, pp. 3238-41.
21. Sindo Kou, David R. Poirier, and Merton C. Flemings: *Metall. Trans. B*, 1978, vol. 9B, pp. 711-19.
22. G.A. Chadwick: *Mater. Sci. Eng.*, 1991, vol. A135, pp. 23-28.